



Supplement of

Measurement report: Online measurement of gas-phase nitrated phenols utilizing a CI-LToF-MS: primary sources and secondary formation

Kai Song et al.

Correspondence to: Song Guo (songguo@pku.edu.cn)

The copyright of individual parts of the supplement might differ from the article licence.

22 **Figures**

23 **Figure S1.** Chemical structures and high-resolution peak fits of reagent ions and
24 nitrated phenols (NPs) investigated in this study.

25 **Figure S2.** (a) Background ions and ions detected during the calibration period
26 (calibrated at the end of the campaign, on Jan 26, 2019); (b) Calibration line of ions (y)
27 and the standard gas-phase concentration of nitrophenol (x). The signals were
28 normalized by reagent ions ($\text{NO}_3^-/(\text{HNO}_3)^{0-2}$).

29 **Figure S3.** The measured concentration of nitrated phenols and their secondary
30 formation simulation by the box model in different model scenarios.

31 **Figure S4.** Air quality and meteorology conditions during the sampling period in
32 Beijing: time series of (a) wind speed, (b) RH, (c) $\text{PM}_{2.5}$, (d) NO_y and (e) CO from Dec
33 1 to Dec 31, 2018.

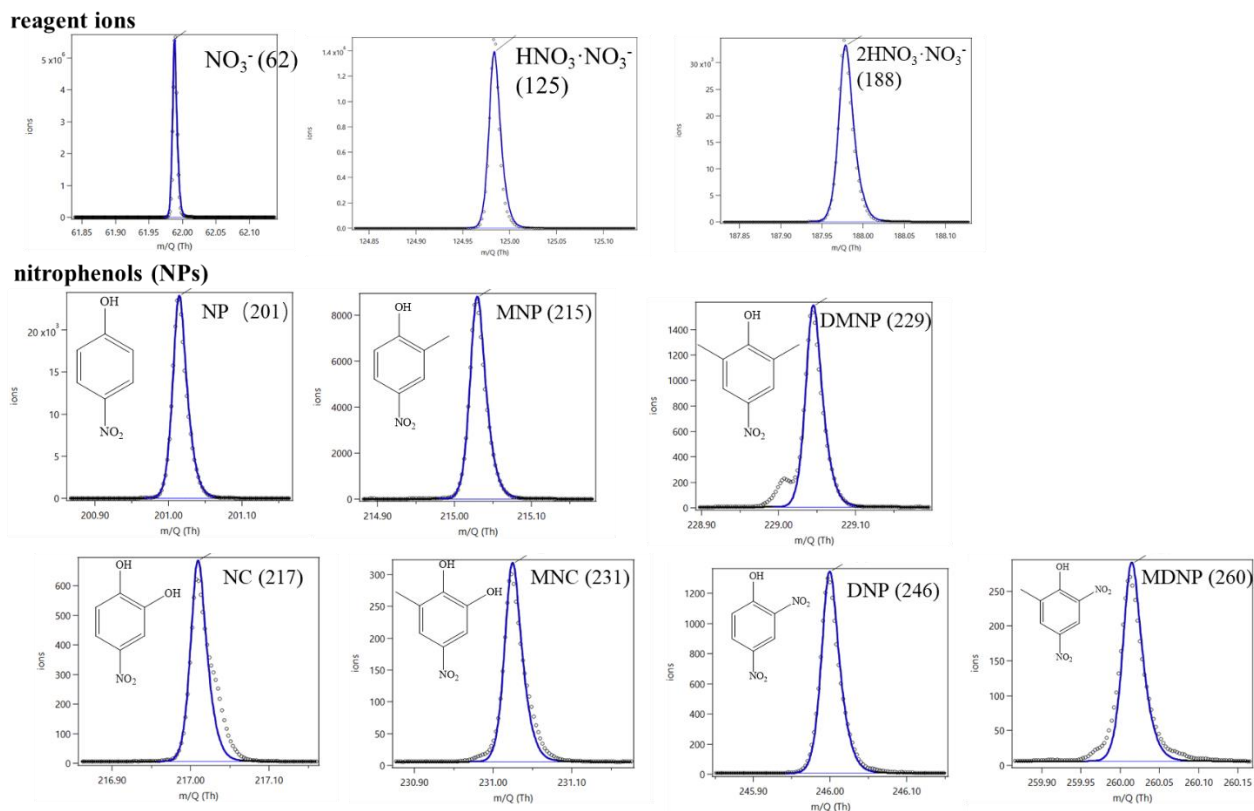
34 **Figure S5.** Consensus maps of brunet, KL, offset, lee, nsNMF and snmf/l algorithms
35 in NMF. The consensus approach was used to estimate the proper method and cluster
36 method of simulation. The color of the consensus map indicated the coefficient and an
37 ideal consensus map was a color-coded heat map in which red blocks along the diagonal
38 on a blue background (Monti et al., 2003; Simpson et al., 2010). KL approach was the
39 optimal one.

40 **Figure S6.** NMF rank survey of factors 3 to 7. The cophenetic coefficient and RSS
41 curves were used for the judgment of factor numbers. The first decreasing cophenetic
42 value (Brunet et al., 2004) and an inflection point of the RSS curve (Hutchins et al.,
43 2008) was the optimal factor number, that was, four factors in this study.

44 **Figure S7.** Diurnal profiles of coal combustion (a), biomass burning (b), industry (c)
45 and vehicle exhaust (d) sources. Coal combustion and biomass burning displayed a
46 nighttime peak while the source of vehicle exhaust showed peaks at rush hour which
47 were evidence of the NMF source apportionment.

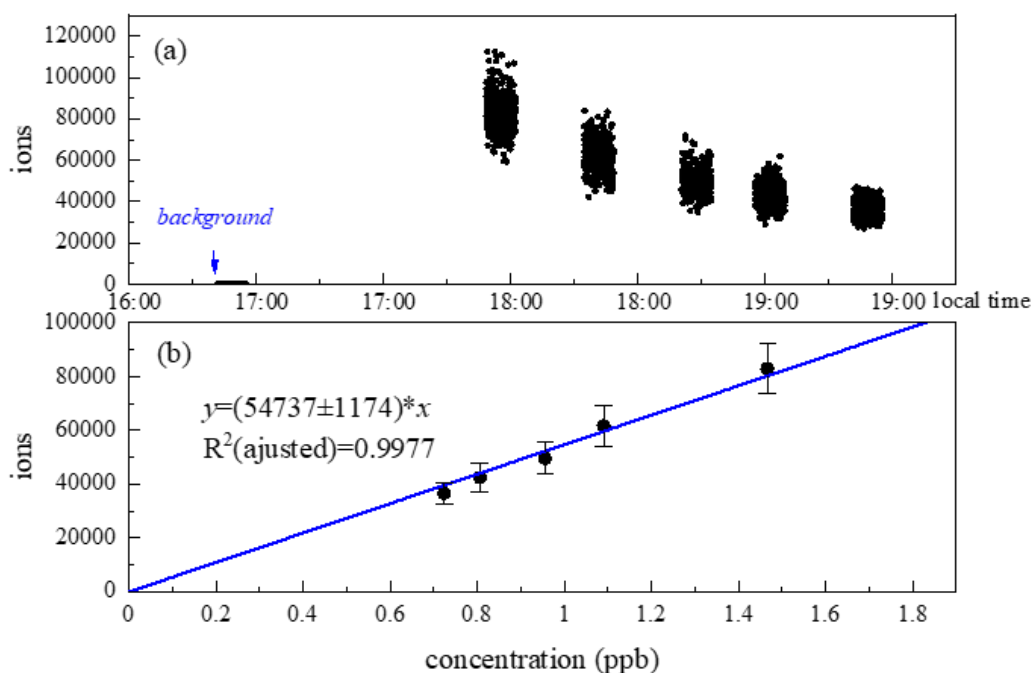
48 **Figure S8.** Source profile from the PMF model. (a) Source profile of PMF results. SO_2 ,
49 chloromethane, aromatics and 1,3-butadiene as the markers of coal combustion,

50 biomass burning, industry and vehicle exhaust sources. (b) Contribution of primary
51 emission (in dark blue borderline) and second formation (in red borderline) of NPs.
52



53
54 Figure S1. Chemical structures and high-resolution peak fits of reagent ions and nitrated
55 phenols (NPs) investigated in this study.

56



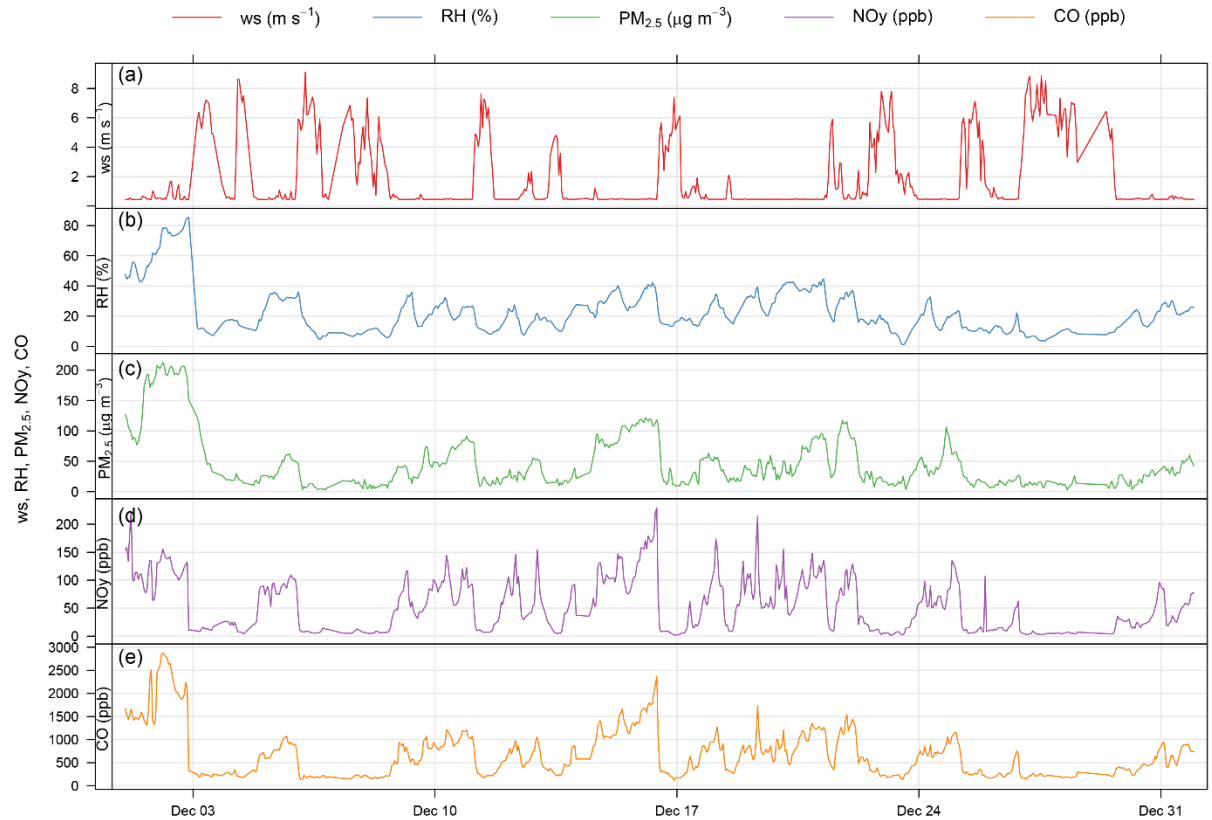
57

58 Figure S2. (a) Background ions and ions detected during the calibration period
 59 (calibrated at the end of the campaign, on Jan 26, 2019); (b) Calibration line of ions (y)
 60 and the standard gas-phase concentration of nitrophenol (x). The signals were
 61 normalized by reagent ions ($\text{NO}_3^- (\text{HNO}_3)_{0-2}$). Yuan et al. calibrated nitrophenol (NP),
 62 methylnitrophenol (MNP) and dinitrophenol (DNP) in the previous study utilizing
 63 nitrate-CIMS. The sensitivity of NP, MNP and DNP were 13.2, 16.6, 10.3 npcs ppt⁻¹,
 64 respectively (Yuan et al., 2016). The sensitivities of MNP and DNP ranged -26% and
 65 22% from NP. Rebecca H. Schwantes et al. estimated sensitivity factors for CIMS
 66 operated in both negative and positive mode using CF_3O^- and $\text{H}_3\text{O}^+(\text{H}_2\text{O})^+$. The
 67 estimated sensitivities of *o*-nitrophenol, 3-nitrocatechol, 4-methyl-2-nitrophenol were
 68 1.48, 1.16 and 1.69, respectively. The sensitivities of NC and MNP ranged 22% and -
 69 14% from NP (Schwantes et al., 2017). Even though uncertainties remain, the addressed
 70 NPs calibrated by NP were correct in concentration levels and magnitudes. Besides, the
 71 secondary formation process simulated by the box model is constrained only by
 72 precursors of NPs measured by online GC-MS rather than the actual concentrations of
 73 NPs. NMF model might be influenced by the uncertainties in the quantification.

74 However, the high time resolution of CIMS increased sample inputs of the NMF model
 75 and reduced the uncertainties for this statistical approach. Even though the actual
 76 contribution of sources faces uncertainties, the proportion of source profiles is still reliable
 77 in this approach.
 78
 79



80
 81 Figure S3. The measured concentration of nitrated phenols and their secondary
 82 formation simulation by the box model in different model scenarios.
 83

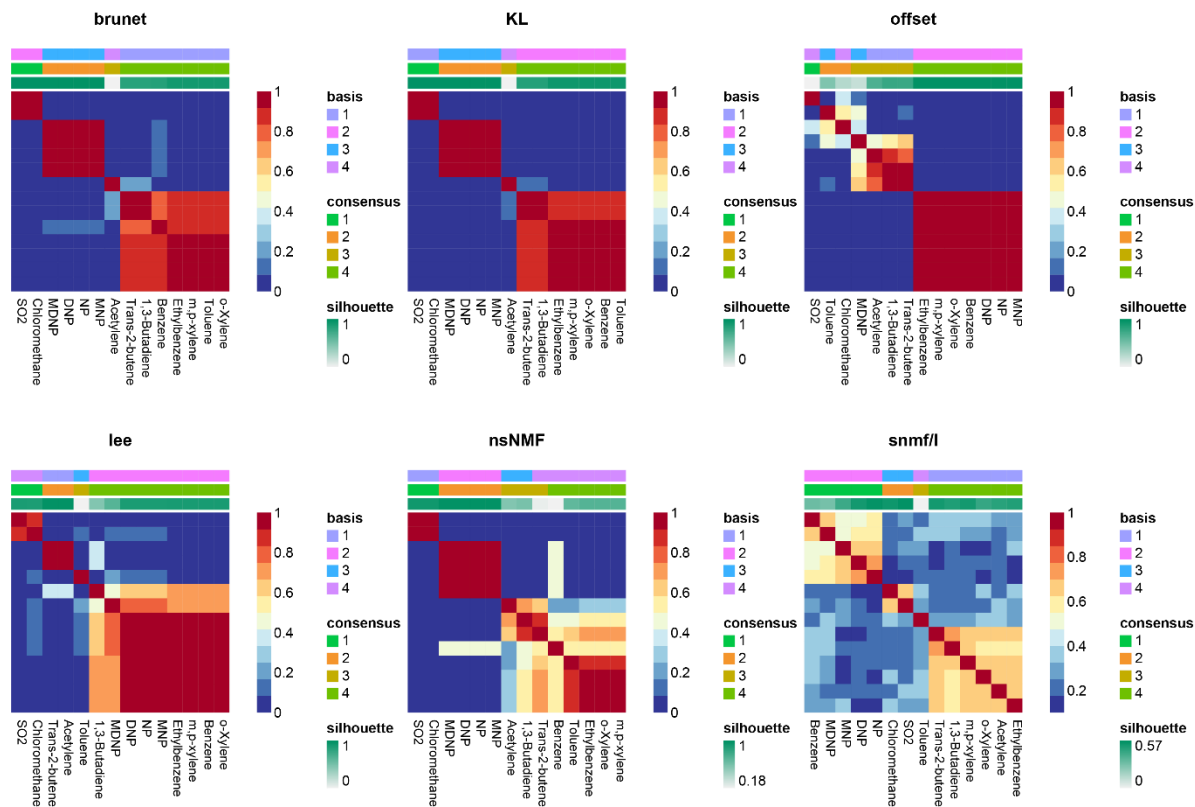


84

85 Figure S4. Air quality and meteorology conditions during the sampling period in
 86 Beijing: time series of (a) wind speed, (b) RH, (c) PM_{2.5}, (d) NO_y and (e) CO from Dec
 87 1 to Dec 31, 2018.

88

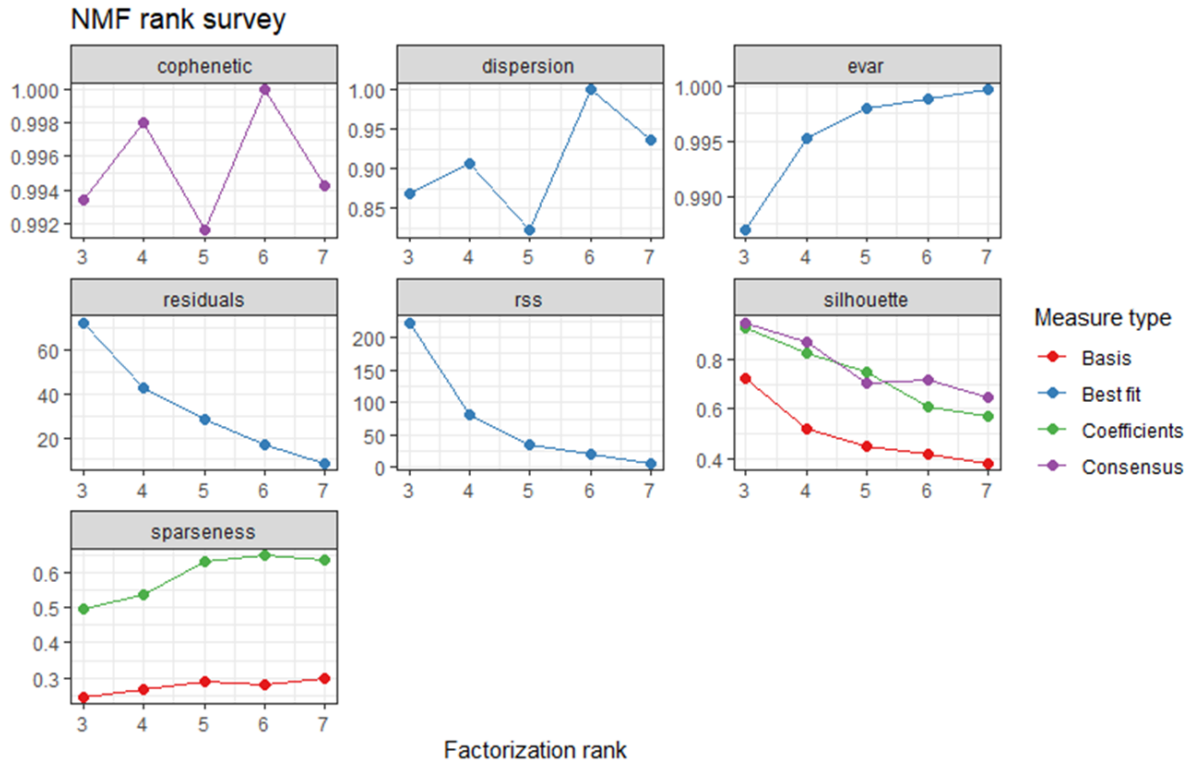
89



90

91 Figure S5. Consensus maps of brunet, KL, offset, lee, nsNMF and snmf/l algorithms in
 92 NMF. The consensus approach was used to estimate the proper method and cluster
 93 method of simulation. The color of the consensus map indicated the coefficient and an
 94 ideal consensus map was a color-coded heat map in which red blocks along the diagonal
 95 on a blue background (Monti et al., 2003; Simpson et al., 2010). KL approach was the
 96 optimal one.

97

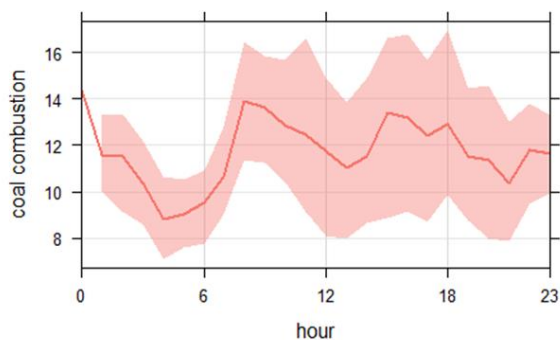


98

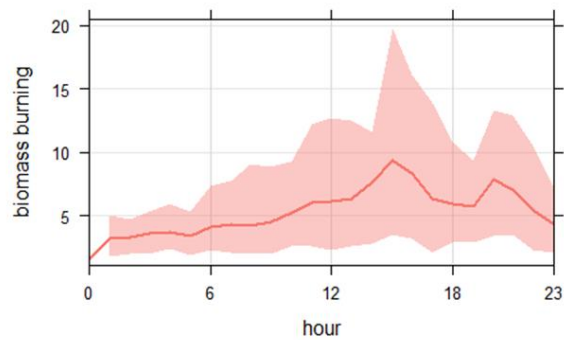
99 Figure S6. NMF rank survey of factors 3 to 7. The cophenetic coefficient and RSS
 100 curves were used for the judgment of factor numbers. The first decreasing cophenetic
 101 value (Brunet et al., 2004) and an inflection point of the RSS curve (Hutchins et al.,
 102 2008) was the optimal factor number, that was, four factors in this study.

103

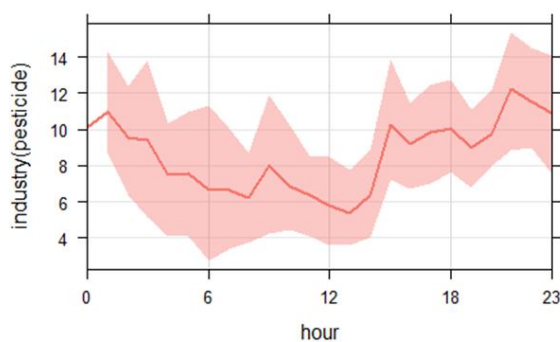
(a) coal combustion



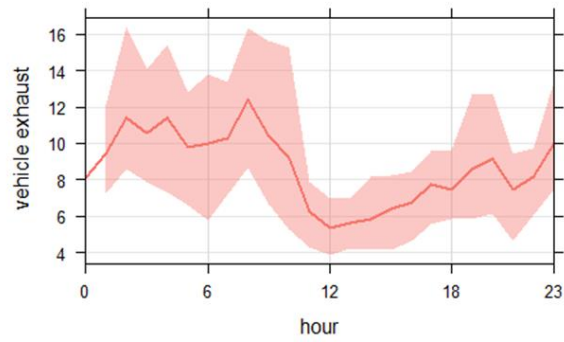
(b) biomass burning



(c) industry



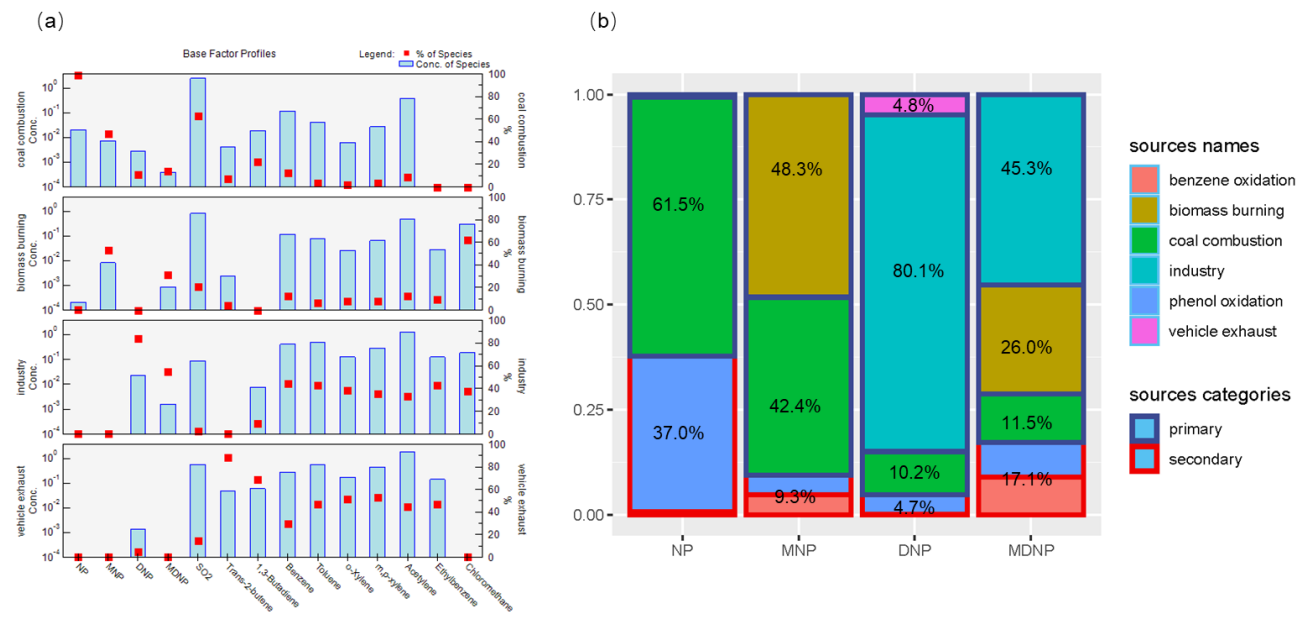
(d) vehicle exhaust



104

105 Figure S7. Diurnal profiles of coal combustion (a), biomass burning (b), industry (c)
106 and vehicle exhaust (d) sources. Coal combustion and biomass burning displayed a
107 nighttime peak while the source of vehicle exhaust showed peaks at rush hour which
108 were evidence of the NMF source apportionment.

109



110

111 Figure S8. Source profile from the PMF model. (a) Source profile of PMF results. SO₂,
 112 chloromethane, aromatics and 1,3-butadiene as the markers of coal combustion,
 113 biomass burning, industry and vehicle exhaust sources. (b) Contribution of primary
 114 emission (in dark blue borderline) and second formation (in red borderline) of NPs.

115

116 **References**

117 Brunet, J. P., Tamayo, P., Golub, T. R. and Mesirov, J. P.: Metagenes and molecular
118 pattern discovery using matrix factorization, *Proc. Natl. Acad. Sci. U. S. A.*,
119 doi:10.1073/pnas.0308531101, 2004.

120 Hutchins, L. N., Murphy, S. M., Singh, P. and Graber, J. H.: Position-dependent motif
121 characterization using non-negative matrix factorization, *Bioinformatics*,
122 doi:10.1093/bioinformatics/btn526, 2008.

123 Monti, S., Tamayo, P., Mesirov, J. and Golub, T.: Consensus clustering: A resampling-
124 based method for class discovery and visualization of gene expression microarray data,
125 *Mach. Learn.*, doi:10.1023/A:1023949509487, 2003.

126 Schwantes, R. H., Schilling, K. A., McVay, R. C., Lignell, H., Coggon, M. M., Zhang,
127 X., Wennberg, P. O. and Seinfeld, J. H.: Formation of highly oxygenated low-volatility
128 products from cresol oxidation, *Atmos. Chem. Phys.*, 17(5), 3453–3474,
129 doi:10.5194/acp-17-3453-2017, 2017.

130 Simpson, T. I., Armstrong, J. D. and Jarman, A. P.: Merged consensus clustering to
131 assess and improve class discovery with microarray data, *BMC Bioinformatics*,
132 doi:10.1186/1471-2105-11-590, 2010.

133 Yuan, B., Liggió, J., Wentzell, J., Li, S. M., Stark, H., Roberts, J. M., Gilman, J., Lerner,
134 B., Warneke, C., Li, R., Leithead, A., Osthoff, H. D., Wild, R., Brown, S. S. and De
135 Gouw, J. A.: Secondary formation of nitrated phenols: Insights from observations
136 during the Uintah Basin Winter Ozone Study (UBWOS) 2014, *Atmos. Chem. Phys.*,
137 16(4), 2139–2153, doi:10.5194/acp-16-2139-2016, 2016.

138